Voronoi Regions of Lattices, Second Moments of Polytopes, and Quantization

J. H. CONWAY AND N. J. A. SLOANE, FELLOW, IEEE

Abstract—If a point is picked at random inside a regular simplex, octahedron, 600-cell, or other polytope, what is its average squared distance from the centroid? In n-dimensional space, what is the average squared distance of a random point from the closest point of the lattice A_n (or D_n, E_n, A_n^* or D_n^*)? The answers are given here, together with a description of the Voronoi (or nearest neighbor) regions of these lattices. The results have applications to quantization and to the design of signals for the Gaussian channel. For example, a quantizer based on the eight-dimensional lattice E_8 has a mean-squared error per symbol of $0.0717 \cdots$ when applied to uniformly distributed data, compared with $0.08333 \cdots$ for the best one-dimensional quantizer.

I. Quantization; Codes for Gaussian Channel

A. Introduction

The MOTIVATION for this work comes from block quantization and from the design of signals for the Gaussian channel. Let us call a finite set of points $y_1, \cdots, y_M$ in n-dimensional Euclidean space $\mathbb{R}^n$ a *Euclidean code*. An n-dimensional *quantizer* with outputs $y_1, \cdots, y_M$ is the function Q: $\mathbb{R}^n \to \mathbb{R}^n$ which sends each point $x \in \mathbb{R}^n$ into $Q(x) =$ closest codepoint y_i (in case of a tie, pick that y_i with the smallest subscript). If x has probability density function $p(x)$, the mean-squared error per symbol of this quantizer is

$$E(n, M, p, \{y_i\}) = \frac{1}{n} \int_{\mathbb{R}^n} \|x - Q(x)\|^2 p(x)\, dx,$$

where $\|x\| = (x \cdot x)^{1/2}$. Around each codepoint y_i is its *Voronoi region* $V(y_i)$ (see [49]), consisting of all points of the underlying space which are closer to that codepoint than to any other. More precisely, we define $V(y_i)$ to be the closed set

$$V(y_i) = \{x \in \mathbb{R}^n \colon \|x - y_i\| \le \|x - y_j\| \text{ for all } j \neq i\}.$$

(Voronoi regions are also called Dirichlet regions, Brillouin zones, Wigner–Seitz cells, or nearest neighbor regions.) If x is an interior point of $V(y_i)$, the quantizer replaces x by $Q(x) = y_i$. Then we may write

$$E(n, M, p, \{y_i\}) = \frac{1}{n} \sum_{i=1}^{M} \int_{V(y_i)} \|x - y_i\|^2 p(x)\, dx. \tag{1}$$

Given n, M, and $p(x)$ one wishes to find the infimum

$$E(n, M, p) = \inf_{\{y_i\}} E(n, M, p, \{y_i\})$$

over all choices of $y_1, \cdots, y_M$. Zador ([53]; see also [6], [7], [24], [52]) showed under quite general assumptions about $p(x)$ that

$$\lim_{M \to \infty} M^{2/n} E(n, M, p) = G_n \left(\int_{\mathbb{R}^n} p(x)^{n/(n+2)}\, dx \right)^{(n+2)/n}, \tag{2}$$

where G_n depends only on n. Zador also showed that

$$\frac{1}{(n+2)\pi} \Gamma\left(\frac{n}{2} + 1\right)^{2/n} \le G_n \le \frac{1}{n\pi} \Gamma\left(\frac{n}{2} + 1\right)^{2/n} \Gamma\left(1 + \frac{2}{n}\right). \tag{3}$$

Asymptotically the upper and lower bounds in (3) agree, giving

$$G_n \to \frac{1}{2\pi e} = 0.0585498 \cdots \text{ as } n \to \infty. \tag{4}$$

Since the probability density function $p(x)$ only appears in the last term of (2), we may choose any convenient $p(x)$ when attempting to find G_n. From now on we assume that the input x is uniformly distributed over a large region in n-dimensional space, and we can usually avoid edge effects by passing to a limiting situation with infinitely many y_i. With this assumption the mean-squared error is minimized if each codepoint y_i lies at the centroid of the corresponding Voronoi region $V(y_i)$ (see [24]). It is known that, for an optimal one-dimensional quantizer with a uniform input distribution, the points y_i should be uniformly spaced along the real line; correspondingly

$$G_1 = \frac{1}{12} = 0.08333 \cdots. \tag{5}$$

Similarly for the optimal two-dimensional quantizer it is known that the points y_i should form the hexagonal lattice

Manuscript received December 7, 1980; revised November 4, 1981.
J. H. Conway is with the Department of Pure Mathematics and Mathematical Statistics, University of Cambridge, 16 Mill Lane, Cambridge CB2 1SB, England.
N. J. A. Sloane is with the Mathematics and Statistics Research Center, Bell Laboratories, Murray Hill, NJ 07974.

0018-9448/82/0300-0211$00.75

A_2 (described in Section III-A); correspondingly

$$G_2 = \frac{5}{36\sqrt{3}} = 0.0801875 \cdots, \tag{6}$$

(see [21], [23], [24], [37]).

In three dimensions Gersho [24] conjectures that the optimal quantizer is based on the body-centered cubic lattice A_3^*, and that

$$G_3 = \frac{19}{192\sqrt[3]{2}} = 0.0785433 \cdots. \tag{7}$$

Similarly in four dimensions he conjectures that the optimal quantizer is based on the lattice D_4, and that

$$G_4 = 0.076602 \tag{8}$$

(obtained by Monte Carlo integration). Furthermore, he conjectures that, in all dimensions, any optimal quantizer is such that for large M the Voronoi regions $V(y_i)$ are all congruent, to some polytope P say. For such a quantizer we obtain, from (1) and (2),

$$G_n = \frac{1}{n} \frac{\int_P \|x - \hat{x}\|^2 \, dx}{\left(\int_P dx\right)^{(n+2)/n}}, \tag{9}$$

where $\hat{x}$ is the centroid of P. The expression on the right makes sense for any polytope and will be denoted by $G(P)$: we refer to it as the *dimensionless second moment of* P. It is also convenient to have symbols for the *volume*, *unnormalized second moment*, and *normalized second moment* of P: these are

$$\mathrm{vol}(P) = \int_P dx,$$

$$U(P) = \int_P \|x - \hat{x}\|^2 \, dx,$$

and

$$I(P) = \frac{U(P)}{\mathrm{vol}(P)},$$

respectively. Then

$$G(P) = \frac{1}{n} \frac{U(P)}{\mathrm{vol}(P)^{1+2/n}} = \frac{1}{n} \frac{I(P)}{\mathrm{vol}(P)^{2/n}}.$$

If Gersho's conjecture is correct then G_n may be determined from

$$G_n = \min_P G(P), \tag{10}$$

taken over all n-dimensional space-filling polytopes. Whether or not the conjecture is true, any value of $G(P)$ for a space-filling polytope is an upper bound to G_n. Furthermore (1), (2) and (9) allow us to interpret G_n and $G(P)$ as *mean-squared quantization errors per symbol*, assuming a uniform input distribution to the quantizer.

In the second application, the same Euclidean code $y_1, \cdots, y_M$ is used as a code for the Gaussian channel. Now the Voronoi regions are the decoding regions: all points x in the interior of $V(y_i)$ are decoded as y_i. If the codewords are equally likely and all the Voronoi regions $V(y_i)$ are congruent to a polytope P, the probability of correct decoding is proportional to

$$\int_P e^{-x \cdot x} \, dx.$$

The description of the Voronoi regions given in Section III thus makes it possible to calculate this probability exactly for many Euclidean codes. These results will be described elsewhere.

B. Summary of Results

In Sections II and III we compute $G(P)$ for a number of important polytopes (not just space-filling ones), including all regular polytopes (see Theorem 4). The three- and four-dimensional polytopes are compared in Tables I and II. The chief tools are Dirichlet's integral (Theorem 1), an explicit formula for the second moment of an n-simplex (Theorem 2), and a recursion formula giving the second moment of a polytope in terms of its cells (Theorem 3).

In Section III we study lattices, in particular the root lattices A_n, D_n, E_6, E_7, E_8, and their duals (defined in Section III-A). We determine the Voronoi regions for these lattices, and their second moments. The second moment gives the average squared distance of a point from the lattice. The *maximum* distance of any point of the underlying space from the lattice is its *covering radius*. The covering radii of these lattices were mostly already known (see for example [2], [4], [31]), but for completeness we rederive them. The final section (Section IV) compares the quantization errors of the different lattices—see Table V and Fig. 20. E_8 is the clear winner.

It is worth mentioning that for most of these lattices there are very fast algorithms for finding the closest lattice point to an arbitrary point; these are described in a companion paper [12]. The sizes of the spherical codes obtained from these lattices have been tabulated in [47].

Although we have tried to keep this paper as self-contained as possible, some familiarity with Coxeter's book [16] will be helpful to the reader. $\mathbb{Z}$ denotes the integers, $\mathbb{Q}$ the rationals and $\mathbb{R}$ the reals.

II. Second Moments of Polytopes

In this section we compute the second moments of a number of fairly simple polytopes; many others will be analyzed in Section III. The methods used are described in Theorems 1–3. A *polytope* in this paper means a convex region of $\mathbb{R}^n$ enclosed by a finite number of hyperplanes (cf. [16, p. 126]). The part of the polytope that lies in one of hyperplanes is called a *cell*. We usually denote the edge-length of our polytopes by $2l$. The main source for information about polytopes is Coxeter [16], but there is an extensive literature, particularly for low-dimensional figures (see for example [1], [13]–[20], [22], [23], [26], [28], [29], [33], [34], [36], [40], [48], and [50]). Although second moments *about an axis* are tabulated for many simple polyhedra in standard engineering handbooks (see also [43]), the results given here appear to be new.

A. Dirichlet's Integral

A few special figures can be handled using Dirichlet's integral.

Theorem 1 ([51, §12.5]): Let f be continuous and $\alpha_1,\cdots,\alpha_n > 0$. Then

$$\int f(x_1+\cdots+x_n)x_1^{\alpha_1}\cdots x_n^{\alpha_n}\frac{dx_1}{x_1}\cdots\frac{dx_n}{x_n} = \frac{\Gamma(\alpha_1)\cdots\Gamma(\alpha_n)}{\Gamma(\alpha_1+\cdots+\alpha_n)}\int_0^1 f(\tau)\tau^{\Sigma\alpha_i-1}\,d\tau,$$

where the integral on the left is taken over the region bounded by $x_1 \geq 0,\cdots,x_n \geq 0$ and $x_1+\cdots x_n \leq 1$.

B. Generalized Octahedron or Crosspolytope

Consider for example the n-dimensional generalized octahedron or crosspolytope β_n [16, p. 121] of edge-length $2l$. Taking $f=1$, $\alpha_1=1$ (to get the volume) or $\alpha_1=3$ (to get the second moment) and $\alpha_i=1$ for $i\geq 2$ in Theorem 1 we find

$$\frac{\operatorname{vol}(\beta_n)}{(2l)^n}=\frac{2^{n/2}}{n!},\quad \frac{I(\beta_n)}{(2l)^2}=\frac{n}{(n+1)(n+2)},$$
$$G(\beta_n)=\frac{(n!)^{2/n}}{2(n+1)(n+2)} \to \frac{1}{2e^2}=0.0676676\cdots \quad \text{as } n\to\infty. \tag{11}$$

C. The n-Sphere

As a second application, for the n-dimensional (solid) sphere S_n of radius ρ we find

$$\frac{\operatorname{vol}(S_n)}{\rho^n}=\frac{\pi^{n/2}}{\Gamma(\frac{1}{2}n+1)},\quad \frac{I(S_n)}{\rho^2}=\frac{n}{n+2},$$
$$G(S_n)=\frac{\Gamma(\frac{1}{2}n+1)^{2/n}}{(n+2)\pi} \to \frac{1}{2\pi e}=0.0585498\cdots \quad \text{as } n\to\infty. \tag{12}$$

It is clear from the definition that the sphere has the smallest value of $G(P)$ of any figure [53]. Thus $G_n \geq G(S_n)$ for all n, which is the sphere lower bound of (3) (see Fig. 20). Unfortunately quantizers cannot be built with either generalized octahedra (for $n\geq 3$) or spheres (for $n\geq 2$) as Voronoi regions, since these objects do not fill space.

D. n-Dimensional Simplexes

The next result makes it possible to find the second moment of any figure provided it can be decomposed into simplexes.

Theorem 2: Let P be an arbitrary simplex in $\mathbb{R}^n$ with vertices $v_i=(v_{i1},\cdots,v_{in})$ for $0\leq i\leq n$. Then

a) the centroid of P is at the barycenter

$$\hat{v}=\frac{1}{n+1}(v_0+\cdots+v_n) \tag{13}$$

of the vertices,

b)

$$\operatorname{vol}(P)=\frac{1}{n!}\det\begin{vmatrix}1 & v_{01} & \cdots & v_{0n}\\ 1 & v_{11} & \cdots & v_{1n}\\ & \cdots & \cdots & \\ 1 & v_{n1} & \cdots & v_{nn}\end{vmatrix}, \tag{14}$$

and

c) the normalized second moment about the origin 0 is

$$I_0=\frac{n+1}{n+2}\|\hat{v}\|^2+\frac{1}{(n+1)(n+2)}\sum_{i=0}^{n}\|v_i\|^2. \tag{15}$$

In other words I_0 is equal to the second moment of a system of $n+1$ particles each of mass $1/(n+1)(n+2)$ placed at the vertices and one particle of mass $(n+1)/(n+2)$ placed at the barycenter.

Proof: a) is elementary, b) is well known (c.f. [25, p. 349]), and c) follows from [25, eq. (24), the case $n=2$].

E. Regular Simplex

For example if P is a regular n-simplex of edge-length $2l$ then

$$\frac{\operatorname{vol}(P)}{(\sqrt{2}\,l)^n}=\frac{\sqrt{n+1}}{n!},\quad \frac{I(P)}{(\sqrt{2}\,l)^2}=\frac{n}{(n+1)(n+2)},$$
$$G(P)=\frac{(n!)^{2/n}}{(n+1)^{1+(1/n)}(n+2)} \to e^{-2}=0.135335\cdots \quad \text{as } n\to\infty. \tag{16}$$

For $n=1$, 2, and 3 the values of $G(P)$ are $1/12$, $1/6\sqrt{3}=0.0962250\cdots$, and $3^{2/3}/20=0.104004\cdots$, and $G(P)$ *increases* monotonically with n.

F. Volume and Second Moment of a Polytope in Terms of its Cells

Instead of decomposing a figure into simplexes one may proceed by induction, expressing the volume and second moment of a polytope in terms of the volume and second moment of its cells, then in terms of its $(n-2)$-dimensional faces, and so on. Theorem 3 is the basis for this procedure.

Suppose P is an n-dimensional polytope with N_1 congruent cells $F_1, F_1', F_1'',\cdots,N_2$ congruent cells $F_2, F_2', F_2'',\cdots$, and so on. Suppose also that P contains a point 0 such that all of the generalized pyramids $0F_1, 0F_1', \cdots$ are congruent, all of $0F_2, 0F_2', \cdots$ are congruent, $\cdots$. Let $\boldsymbol{a}_i \in F_i$ be the foot of the perpendicular from 0 to F_i, let $h_i = \|0\boldsymbol{a}_i\|$, and let $V_{n-1}(i)$ be of volume of F_i and $U_{n-1}(i)$ the unnormalized second moment of F_i about $\boldsymbol{a}_i$.

Theorem 3: The volume and unnormalized second moment about 0 of P are given by

$$\mathrm{vol}(P) = \sum_i \frac{N_i h_i}{n} V_{n-1}(i),$$

$$U(P) = \sum_i \frac{N_i h_i}{n+2}\left[h_i^2 V_{n-1}(i) + U_{n-1}(i)\right].$$

Proof: Follows from elementary calculus by dividing each generalized pyramid $0F_i$ into slabs parallel to the cell F_i.

G. Truncated Octahedron

For example let P be the truncated octahedron with vertices consisting of all permutations of $\sqrt{2}\,l(0, \pm 1, \pm 2)$. P has $N_1 = 6$ square cells and $N_2 = 8$ cells which are regular hexagons, all with edge-length $2l$. The second moments of these cells can be calculated directly, or else found in Section II-I below. Then from the theorem we find that

$$\mathrm{vol}(P) = \frac{6 \cdot l\sqrt{8}}{3} 4l^2 + \frac{8 \cdot l\sqrt{6}}{3} 6\sqrt{3}\,l^2 = 64\sqrt{2}\,l^3,$$

$$U(P) = \frac{6 \cdot l\sqrt{8}}{5}\left[8l^2 \cdot 4l^2 + \frac{8l^4}{3}\right] + \frac{8 \cdot l\sqrt{6}}{5}\left[6l^2 \cdot 6\sqrt{3}\,l^2 + 10\sqrt{3}\,l^4\right] = 304\sqrt{2}\,l^5,$$

hence

$$I(P) = \frac{U(P)}{\mathrm{vol}(P)} = \frac{19 l^4}{4},$$

$$G(P) = \frac{1}{3}\frac{I(P)}{\mathrm{vol}(P)^{2/3}} = \frac{19}{192^3\sqrt{2}} = 0.0785433 \cdots. \tag{17}$$

H. Second Moment of Regular Polytopes

The next theorem gives an explicit formula for the second moment of any regular polytope. Suppose P is an n-dimensional regular polytope [16]. For $0 \le j \le n$ choose a j-dimensional face F_j of P so that $F_0 \subseteq F_1 \cdots \subseteq F_n = P$, and let 0_j be the center of F_j, $R_j = \|0_n 0_j\|$, and for $j \ge 1$ let $r_j = \|0_{j-1}0_j\|$. Thus r_j is the inradius of F_j measured from 0_j, and $r_j^2 = R_{j-1}^2 - R_j^2$. Let $N_{j,j-1}$ be the number of $((j-1)$-dimensional) cells of F_j. Then it is known that the symmetry group of P has order

$$g = N_{n,n-1}N_{n-1,n-2}\cdots N_{2,1}N_{1,0}$$

(see [16, p. 130]), and that the volume of P is

$$\mathrm{vol}(P) = N_{n,n-1}\cdots N_{2,1}N_{1,0}\cdot\frac{r_1 r_2 \cdots r_n}{n!} \tag{18}$$

(see [16, p. 137]).

Theorem 4: The second moment of any n-dimensional regular polytope P about its center 0_n is given by

$$I(P) = \frac{2}{(n+1)(n+2)} \cdot \left(R_0^2 + 2R_1^2 + 3R_2^2 + \cdots + nR_{n-1}^2\right) \tag{19}$$

or equivalently

$$I(P) = \frac{2}{(n+1)(n+2)} \cdot \left(r_1^2 + 3r_2^2 + 6r_3^2 + \cdots + \frac{n(n+1)}{2}r_n^2\right). \tag{20}$$

Proof: The proof is by induction, the one-dimensional case being immediate. From Theorem 3 we have

$$U(P) = \frac{N_{n,n-1}r_n}{n+2}\left[r_n^2 V_{n-1}(P) + U_{n-1}(P)\right],$$

where (from (18) and the induction hypothesis)

$$V_{n-1}(P) = N_{n-1,n-2}\cdots N_{2,1}N_{1,0}\cdot\frac{r_1 r_2\cdots r_{n-1}}{(n-1)!},$$

$$U_{n-1}(P) = V_{n-1}(P) \cdot \frac{2}{n(n+1)}\left[r_1^2 + \cdots + \frac{n(n-1)}{2}r_{n-1}^2\right].$$

Then

$$I(P) = \frac{U(P)}{\mathrm{vol}(P)} = \frac{n}{n+2}\left[r_n^2 + \frac{2}{n(n+1)} \cdot \left(r_1^2 + \cdots + \frac{n(n-1)}{2}r_{n-1}^2\right)\right]$$

which simplifies to (20).

The values of g, $\mathrm{vol}(P)$ and R_j are tabulated for all regular polytopes in [16, table I, pp. 292–295]. We have already dealt with the simplex and generalized octahedron. For an n-dimensional cube $G(P) = 1/12$ for all n (since the cube is a direct product of line segments). We now treat the remaining regular polytopes.

I. Regular Polygons

If P is a regular p-gon of edge-length $2l$ then from Theorem 4 we find

$$\mathrm{vol}(P) = pl^2\cot\frac{\pi}{p},$$

$$I(P) = \frac{l^2}{6}\left(1 + 3\cot^2\frac{\pi}{p}\right),$$

$$G(P) = \frac{1}{6p}\left(\mathrm{cosec}\frac{2\pi}{p} + \cot\frac{\pi}{p}\right). \tag{21}$$

For $p = 3, 4$, and 6, $G(P) = 1/6\sqrt{3}$, $1/12$, and $5/36\sqrt{3}$.

J. Icosahedron and Dodecahedron

For the icosahedron

$$\mathrm{vol} = \frac{20l^3\tau^2}{3}, \quad I = \frac{3l^2\tau^2}{5},$$

$$G = \frac{1}{20}\left(\frac{6\tau}{5}\right)^{2/3} = 0.0778185 \cdots, \tag{22}$$

where $\tau = (\sqrt{5}+1)/2$, and for the dodecahedron

$$\mathrm{vol} = 4\sqrt{5}\, l^3\tau^4, \quad I = l^2 \cdot \frac{39\tau + 28}{25},$$

$$G = \frac{11\tau + 17}{300}\left(\frac{2}{\tau\sqrt{5}}\right)^{2/3} = 0.0781285 \cdots. \tag{23}$$

K. The Exceptional Four-Dimensional Polytopes

There are three "exceptional" regular polytopes in four dimensions, the 24-cell, the 120-cell, and the 600-cell (the prefix giving the number of cells—see [16]). For the 24-cell

$$\mathrm{vol} = 32l^4, \quad I = 26l^2/15,$$

$$G = \frac{13}{120\sqrt{2}} = 0.0766032 \cdots; \tag{24}$$

for the 120-cell

$$\mathrm{vol} = 120\sqrt{5}\, l^4\tau^8, \quad I = \frac{2l^2}{15\sqrt{5}}\left(282 + 127\sqrt{5}\right),$$

$$G = \frac{43\tau + 13}{300\sqrt{6}\, 5^{1/4}} = 0.0751470 \cdots; \tag{25}$$

and for the 600-cell

$$\mathrm{vol} = 100l^4\tau^3, \quad I = \frac{4l^2}{15}\left(12 + 5\sqrt{5}\right),$$

$$G = \frac{(3\tau + 4)\tau^{1/2}}{150} = 0.0750839 \cdots. \tag{26}$$

L. Comparisons

The three- and four-dimensional polytopes that have been considered are compared in Tables I and II.

TABLE I
COMPARISON OF DIMENSIONLESS SECOND MOMENT $G(P)$ FOR VARIOUS THREE-DIMENSIONAL POLYHEDRA P

P	G(P)
tetrahedron	.1040042 ...
cube*	.0833333 ...
octahedron	.0825482 ...
hexagonal prism*	.0812227 ...
rhombic dodecahedron*	.0787451 ...
truncated octahedron*	.0785433 ...
dodecahedron	.0781285 ...
icosahedron	.0778185 ...
sphere	.0769670 ...

*A space-filling polyhedron.

TABLE II
COMPARISON OF DIMENSIONLESS SECOND MOMENT $G(P)$ FOR VARIOUS FOUR-DIMENSIONAL POLYTOPES P

P	G(P)
simplex	.1092048 ...
cube*	.0833333 ...
generalized octahedron	.0816497 ...
24-cell*	.0766032 ...
120-cell	.0751470 ...
600-cell	.0750839 ...
sphere	.0750264 ...

*A space-filling polytope.

III. VORONOI REGIONS OF LATTICES AND THE MEAN-SQUARE ERROR OF LATTICE QUANTIZERS

In this section we determine the Voronoi regions of various n-dimensional lattices, and their volumes and second moments. Since these lattices can be used to construct n-dimensional quantizers for uniformly distributed inputs, the dimensionless second moments give upper bounds to G_n (see (10) and Section IV). The lattices considered are the *root lattices*[1] and their duals, namely A_n, A_n^*, D_n, D_n^*, E_6, E_7, and E_8 (we shall not consider E_6^* or E_7^* here, while $E_8^* = E_8$).

[1]A root lattice is a lattice spanned by the root system of a Lie algebra—see [5], [30].

For general information about lattices see for example [4], [5], [8], [11], [14]–[17], [28], [32], [38], [39], and [45]–[47]. In particular if Λ is a lattice in $\mathbb{R}^n$ the *dual* (or *reciprocal* or *polar*) lattice Λ^* consists of all points x in the span $\mathbb{Q}\Lambda$ such that $x \cdot y \in \mathbb{Z}$ for all $y \in \Lambda$. Since all the points in a lattice are equivalent, it is enough to find the Voronoi region around the origin, i.e., the closed set

$$V(0) = \{x \in \mathbb{R}^n \mid \|x\| \le \|x - u\| \text{ for all nonzero } u \in \Lambda\}.$$

The volume of the Voronoi region can be written down immediately from the other standard parameters of the lattice:

$$\mathrm{vol}\, V(0) = \frac{V_n\rho^n}{\Delta} = \frac{\rho^n}{\delta} = \sqrt{d}, \tag{27}$$

where V_n is the volume of a unit sphere in $\mathbb{R}^n$, 2ρ is the minimum distance between the points of Λ, and Δ, δ and d are respectively the density, center density, and determinant of Λ. The covering radius will be denoted by R_c.

A. Definition of the Root Lattices

For $n \geq 1$, A_n is the n-dimensional[2] lattice consisting of the points $(x_0, x_1, \cdots, x_n)$ in $\mathbb{Z}^{n+1}$ with $\Sigma x_i = 0$. The dual A_n^* consists of the union of $n+1$ cosets of A_n:

$$A_n^* = \bigcup_{i=0}^{n} ([i] + A_n),$$

where

$$[i] = \left(\frac{-j}{n+1}, \frac{-j}{n+1}, \cdots, \frac{-j}{n+1}, \frac{i}{n+1}, \cdots, \frac{i}{n+1}\right)$$
$$= \left(\left(\frac{-j}{n+1}\right)^i, \left(\frac{i}{n+1}\right)^j\right) \tag{28}$$

and $i + j = n + 1$. For $n = 1$ and 2, $A_n^* \cong A_n$ (i.e., they differ only by a rotation and change of scale).

For $n \geq 2$, D_n consists of the points $(x_1, x_2, \cdots, x_n)$ in $\mathbb{Z}^n$ with Σx_i even. In other words, if we color the integer lattice points alternately red and blue in a checkerboard coloring, D_n consists of the red points. The dual D_n^* is the union of four cosets of D_n:

$$D_n^* = \bigcup_{j=0}^{3} ([i] + D_n),$$

where

$$[0] = (0^n), \quad [1] = \left(\tfrac{1}{2}^n\right),$$
$$[2] = (0^{n-1}, 1), \quad [3] = \left(\tfrac{1}{2}^{n-1}, -\tfrac{1}{2}\right).$$

Also $D_2 \cong A_1 \oplus A_1$, $D_3 \cong A_3$, and $D_4^* \cong D_4$. Equivalently, D_n may be obtained by applying Construction A of [32] or [45] to the even weight code of length n. Similarly D_n^* is obtained by applying Construction A to the dual code $\{0^n, 1^n\}$.

There are many possible definitions of the lattices E_6, E_7, and E_8 (see the references given at the beginning of this section). We shall use the following: E_8 is the union of D_8 and the coset

$$\left(\tfrac{1}{2}, \tfrac{1}{2}, \tfrac{1}{2}, \tfrac{1}{2}, \tfrac{1}{2}, \tfrac{1}{2}, \tfrac{1}{2}, \tfrac{1}{2}\right) + D_8.$$

In other words E_8 consists of the points $(x_1, \cdots, x_8)$ with $x_i \in \mathbb{Z}$ and Σx_i even, together with the points $(y_1, \cdots, y_8)$ with $y_i \in \mathbb{Z} + \frac{1}{2}$ and Σy_i even. E_7 is a subspace of dimension 7 in E_8, consisting of the points $(u_1, \cdots, u_8) \in E_8$ with $u_7 = -u_8$. E_6 is a subspace of dimension 6 in E_8, consisting of the points $(u_1, \cdots, u_8) \in E_8$ with $u_6 = u_7 = -u_8$.

B. Voronoi Region of a Root Lattice

In this section we give a uniform method for finding the Voronoi region of any root lattice Λ (the dual lattices must be handled differently). The method is based on finding a fundamental simplex for the affine Weyl group of the lattice (cf. [3], [5], [16]).

[2]The subscript gives the dimension of the lattice.

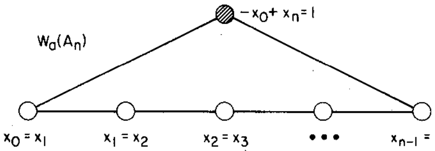

Fig. 1. Extended Coxeter–Dynkin diagram for $W_a(A_n)$. The extending node is indicated by a solid circle. The $n+1$ nodes are labeled with the equations to the hyperplanes which are the walls of the fundamental simplex. The labelings in Fig. 1–3 are based on [5, pp. 250–2100] and [10].

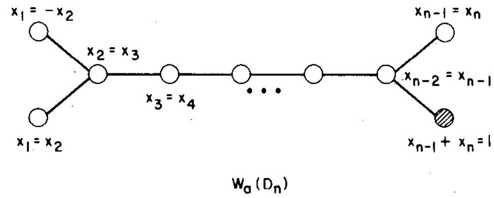

Fig. 2. Extended Coxeter–Dynkin diagram for $W_a(D_n)$. There are $n+1$ nodes.

The (ordinary) *Weyl group* $W(\Lambda)$ of an n-dimensional root lattice Λ is a certain finite group of orthogonal transformations of $\mathbb{R}^n$ which sends Λ to itself (for the precise definition see [5, p. 143] or [30, p. 43]).[3] Similarly the *affine Weyl group* $W_a(\Lambda)$ is a certain infinite group of isometries of $\mathbb{R}^n$ which sends Λ to itself (see [5, p. 173]); and $W(\Lambda)$ is the subgroup of $W_a(\Lambda)$ fixing the origin.[4] The affine Weyl group is described by the extended Coxeter–Dynkin diagram shown in Figs. 1–3.

This diagram can be read in at least three different ways (see [3], [5], [16], [27]). First, it provides a presentation for $W_a(\Lambda)$, defining the group in terms of generators and relations; however we shall not make use of this interpretation here. Second, it can be used to specify a *fundamental simplex* S for $W_a(\Lambda)$. This is an n-dimensional closed simplex whose images under the action of $W_a(\Lambda)$ are distinct and tile $\mathbb{R}^n$. In other words we can write

$$\mathbb{R}^n = \bigcup_{g \in W_a(\Lambda)} g(S), \tag{29}$$

where (except for the boundaries of $g(S)$, a set of measure zero) each point $x \in \mathbb{R}^n$ belongs to a unique $g(S)$. In this interpretation the nodes of the diagram represent the hyperplanes which are the walls of the fundamental simplex [16, p. 191]. The angle between two walls or hyperplanes is indicated by the branch of the diagram joining the corresponding nodes. If the hyperplanes are at an angle of $\pi/3$ the nodes are joined by a single branch, if the angle is $\pi/4$ they are joined by a double branch (see Fig. 4), if the angle is π/p with $p > 4$ they are joined by a branch labeled p, and finally if the hyperplanes are perpendicular the nodes

[3]$W(\Lambda)$ is generated by the reflections in the hyperplanes through the origin perpendicular to the minimal vectors of the lattice. Alternatively, in the terminology of [11], $W(\Lambda)$ is the group $G_0(\Lambda)$, while the full group of orthogonal transformations sending Λ to itself is a split extension of $G_0(\Lambda)$ by $G_1(\Lambda)$.

[4]We may think of Λ itself as being an Abelian group of translations of $\mathbb{R}^n$, which sends Λ to Λ. Then $W_a(\Lambda)$ is a split extension of Λ by $W(\Lambda)$.

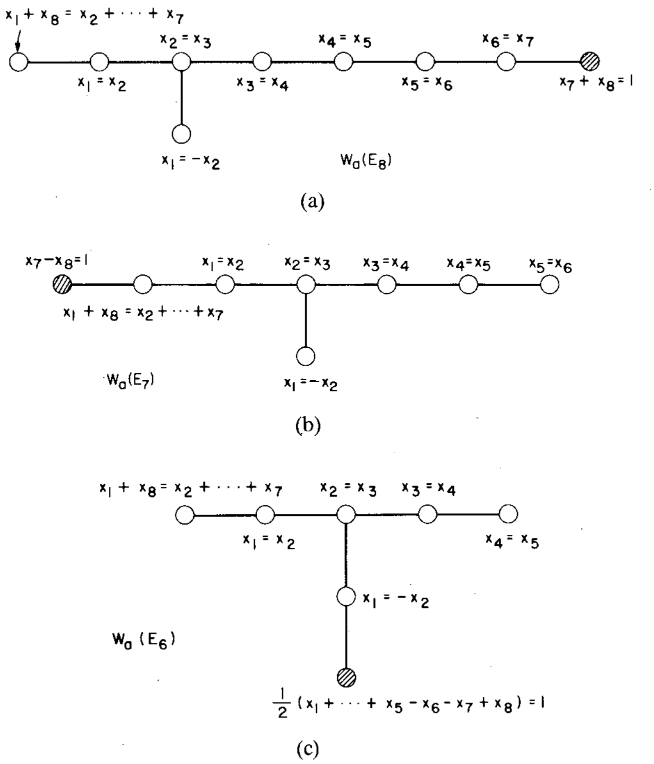

Fig. 3. Extended Coxeter–Dynkin diagrams for (a) $W_a(E_8)$, (b) $W_a(E_7)$, and (c) $W_a(E_6)$.

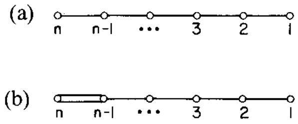

Fig. 4. Coxeter–Dynkin diagrams for the spherical simplexes of (a) $W(A_n)$ and (b) $W(C_n)$. (The labeling of the nodes is for convenience only and has no geometrical significance.)

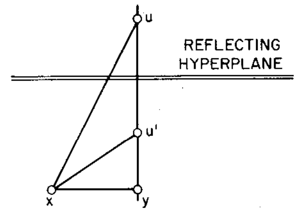

Fig. 5.

are not joined by a branch. The nodes in Figs. 1–3 have been labeled with the equations to the corresponding hyperplanes.

In the third interpretation the nodes in the extended Coxeter–Dynkin diagram are taken to represent the *vertices* of a fundamental simplex, rather than the bounding hyperplanes. Each node represents the vertex opposite to the corresponding hyperplane (some examples are shown in Figs. 6, 8, and 9)—see [16, p. 196].

One of the nodes in the diagram is indicated by a solid circle. This is the *extending node*; removing it leaves a Coxeter–Dynkin diagram for the Weyl group $W(\Lambda)$. Of the $n+1$ hyperplanes represented by the extended diagram, all except that corresponding to the extending node pass through the origin. It is helpful to think of the latter hyperplane as forming the *roof* of the fundamental simplex. The vertex of the fundamental simplex opposite the roof is the origin.

For later use we remark that the finite Weyl group $W(\Lambda)$ also has a fundamental domain, consisting of an infinite cone centered at the origin. A fundamental simplex for $W_a(\Lambda)$ is obtained by taking the finite part of the cone beneath the roof. The intersection of this cone with the roof, or more precisely with a unit sphere centered at the origin, is a *spherical simplex*. The Coxeter–Dynkin diagram for $W(\Lambda)$—i.e., with the extending node deleted—describes this spherical simplex in the same way as the extended diagram describes the fundamental simplex for $W_a(\Lambda)$. These spherical simplexes and (unextended) Coxeter–Dynkin diagrams can be used to define the Weyl groups of all the root *systems* (and not just the root *lattices* A_n, D_n, and E_n). In Sections F and G we shall require the spherical simplexes corresponding to $W(A_n)$ and $W(C_n)$, shown in Fig. 4. The Weyl group $W(A_n)$ is usually written as $[3^{n-1}]$ and is isomorphic to the symmetric group on $n+1$ letters. $W(C_n)$ is written $[3^{n-2}, 4]$ and has order $2^n n!$. (See [3], [5], [16], [18], and [30].)

Lemma: The origin is the closest lattice point to any interior point of the fundamental simplex.

Proof: Let $\boldsymbol{u}$ be the closest lattice point to $\boldsymbol{x} \in S$. Suppose $\boldsymbol{u} \neq 0$. Then $\boldsymbol{u} \notin S$, and $\boldsymbol{u}$ and $\boldsymbol{x}$ are on opposite sides of a reflecting hyperplane of $W_a(\Lambda)$. Let $\boldsymbol{u}' \in \Lambda$ be the image of $\boldsymbol{u}$ in this hyperplane, and let $\boldsymbol{y}$ be the foot of the perpendicular from $\boldsymbol{x}$ to the line $\boldsymbol{uu}'$ (see Fig. 5). Then $\|\boldsymbol{xu}'\|^2 = \|\boldsymbol{xy}\|^2 + \|\boldsymbol{yu}'\|^2 < \|\boldsymbol{xy}\|^2 + \|\boldsymbol{yu}\|^2 = \|\boldsymbol{xu}\|^2$, and $\boldsymbol{x}$ is closer to $\boldsymbol{u}'$ than to $\boldsymbol{u}$, a contradiction. Therefore $\boldsymbol{u} = 0$.

The connection between the fundamental simplex and the Voronoi region is given by the following basic theorem.

Theorem 5: For any root lattice Λ, the Voronoi region around the origin is the union of the images of the fundamental simplex under the Weyl group $W(\Lambda)$.

Proof: Let $\boldsymbol{x}$ be any point of the Voronoi region around the origin. From (29), $\boldsymbol{x} \in g(S)$ for some $g \in W_a(\Lambda)$. Suppose $\boldsymbol{x}$ is an interior point of $g(S)$. By the lemma, the closest lattice point to $\boldsymbol{x}$ is $g(0)$. Therefore $g(0) = 0$, $g \in W(\Lambda)$, and

$$\boldsymbol{x} \in \bigcup_{g \in W(\Lambda)} g(S).$$

We omit the discussion of the case when $\boldsymbol{x}$ is a boundary point of $g(S)$. The converse statement, that $\boldsymbol{x} \in \cup g(S)$ implies $\boldsymbol{x}$ is in the Voronoi region, follows by reversing the steps.

It follows from Theorem 5 that the Voronoi region is the union of $|W(\Lambda)|$ copies of the fundamental simplex S. Furthermore the cells of the Voronoi region are the images of the roof of the fundamental simplex under $W(\Lambda)$. Thus the Voronoi region is bounded by hyperplanes which are the perpendicular bisectors of the lines joining 0 to its nearest neighbors in the lattice.

Corollary: The number of $(n-1)$-dimensional cells of the Voronoi region of a root lattice is equal to the contact number of the lattice (the number of nearest neighbors of any lattice point).

This is not true for all lattices, as we shall see in Section III-H.

The second moment of the Voronoi region can now be obtained from that of the fundamental simplex. The results are given in the following sections.

C. Voronoi Region for A_n

We first find the vertices $v_0, v_1, \cdots, v_n$ of the fundamental simplex S. These are found by omitting each of the hyperplanes of Fig. 1 in turn and calculating the point of intersection of the remaining n hyperplanes. The results are shown in Fig. 6, where each node is labeled with the coordinates of the vertex opposite the corresponding hyperplane. The ith vertex is

$$v_i = \left(\left(-\frac{j}{n+1} \right)^i \left(\frac{i}{n+1} \right)^j \right)$$

where $i + j = n + 1$, for $0 \le i \le n$, and is the same as the coset representative $[i]$ for A_n in A_n^* (see (28)). Also

$$\| v_i \|^2 = \frac{ij}{n+1}. \tag{30}$$

The barycenter of S (13) is

$$\begin{aligned} \hat{v} &= \frac{1}{n+1} \sum_{i=0}^{n} v_i \\ &= \left(\frac{-n}{2n+2}, \frac{-n+2}{2n+2}, \cdots, \frac{n-2}{2n+2}, \frac{n}{2n+2} \right) \end{aligned}$$

and from (15) the normalized second moment about the origin is

$$\begin{aligned} I(S) &= \frac{n+1}{n+2} \| \hat{v} \|^2 + \frac{1}{(n+1)(n+2)} \sum_{i=0}^{n} \| v_i \|^2 \\ &= \frac{n+1}{n+2} \cdot \frac{n(n+2)}{12(n+1)} + \frac{1}{(n+1)(n+2)} \cdot \frac{n(n+2)}{6} \\ &= \frac{n}{12} + \frac{n}{6(n+1)}. \end{aligned}$$

Now $|W(A_n)| = (n+1)!$ and the determinant d is $n+1$ [5, pp. 250–251]. By Theorem 5 the Voronoi region around the origin, $V(0)$, is the union of $|W(A_n)|$ copies of S, so

$$\begin{aligned} I(V(0)) &= \frac{U(V(0))}{\mathrm{vol}(V(0))} \\ &= \frac{|W(A_n)| \cdot U(S)}{|W(A_n)| \cdot \mathrm{vol}(S)} \\ &= \frac{U(S)}{\mathrm{vol}(S)} = I(S). \end{aligned} \tag{31}$$

Also $\mathrm{vol}(V(0)) = \sqrt{n+1}$ from (27). Therefore the dimensionless second moment of the Voronoi region of A_n is

$$\begin{aligned} G(A_n) &= \frac{1}{n} \frac{I(V(0))}{\mathrm{vol}(V(0))^{2/n}} \\ &= \frac{1}{(n+1)^{1/n}} \left(\frac{1}{12} + \frac{1}{6(n+1)} \right) \\ &\to \frac{1}{12} \qquad \text{as } n \to \infty. \end{aligned} \tag{32}$$

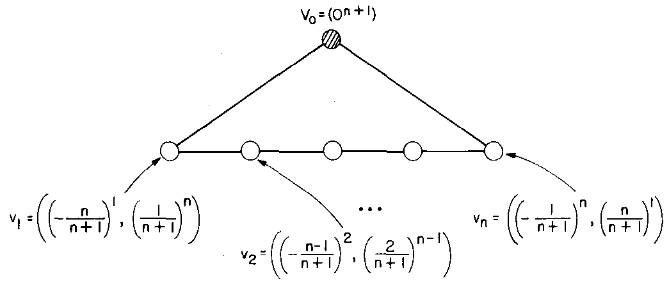

Fig. 6. Vertices of fundamental simplex for A_n.

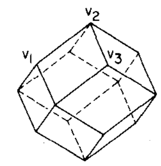

Fig. 7. A rhombic dodecahedron, the Voronoi region $V(0)$ for the face-centered cubic lattice A_3. The points v_0 (not shown, but at the center of the figure), v_1, v_2, and v_3 form a fundamental simplex S, and the rhombic dodecahedron is the union of 24 copies of S.

Once the Voronoi region has been found we can also determine the points in $\mathbb{R}^n$ at maximum distance from the lattice, since these are necessarily vertices of the Voronoi regions. From (30) it follows that the covering radius of A_n (the maximum distance of any point in $\mathbb{R}^n$ from A_n) is

$$R_c = \sqrt{\frac{ab}{n+1}} = \rho \sqrt{\frac{2ab}{n+1}},$$

where ρ is the packing radius (see (27)) and $a = [(n+1)/2]$, $b = n + 1 - a$. Typical points at this distance from A_n are the vertex v_a of $V(0)$ and its images under $W(A_n)$.

The lattice A_1 consists of equally spaced points on the real line, and $G(A_1) = 1/12$. The lattice A_2 is the hexagonal lattice, the fundamental simplex is an equilateral triangle, the Voronoi region is a hexagon, and $G(A_2) = 5/36\sqrt{3}$ (compare Section II-I). The lattice A_3 is the face-centered cubic lattice, the densest known sphere packing in $\mathbb{R}^3$, the Voronoi region is a rhombic dodecahedron (Fig. 7; see also [33, p. 130] and [22, p. 294 and anaglyph XI]), and $G(A_3) = 2^{-11/3} = 0.0787451 \cdots$.

For $n = 1$ and 2 it is known that A_n is the optimal quantizer (see (5) and (6)), but for $n = 3$ the dual lattice A_3^* is better. The values of $G(A_n)$ for $n \le 9$ are plotted in Fig. 20. $G(A_n)$ decreases to its minimum value of $0.0773907 \cdots$ at $n = 8$ and then slowly increases to $1/12$ as $n \to \infty$.

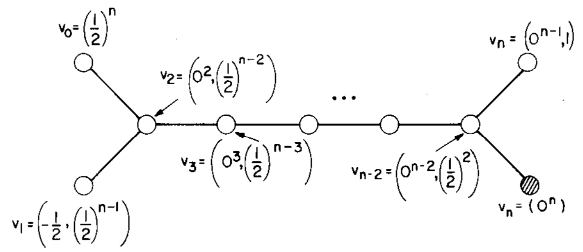

Fig. 8. Vertices of fundamental simplex for D_n.

D. Voronoi Region for D_n ($n \geq 4$)

D_n (for $n \geq 4$), E_6, E_7, and E_8 are handled in the same way as A_n and our treatment will be brief. The vertices $v_0, \cdots, v_n$ of a fundamental simplex for D_n, $n \geq 4$, are shown in Fig. 8. Their barycenter is

$$\hat{v} = \frac{1}{2(n+1)}(0, 2, 3, \cdots, n-2, n-1, n+1),$$

$|W(D_n)| = 2^{n-1} \cdot n!$ and the determinant $d = 4$. For the Voronoi region $V(0)$ we find

$$I(V(0)) = \frac{n}{12} + \frac{1}{2(n+1)},$$

$$\mathrm{vol}(V(0)) = 2,$$

and

$$G(D_n) = \frac{1}{2^{2/n}}\left(\frac{1}{12} + \frac{1}{2n(n+1)}\right) \rightarrow \frac{1}{12} \quad \text{as } n \rightarrow \infty. \tag{33}$$

The covering radius of D_n (for $n \geq 4$) is

$$R_c = \sqrt{\frac{n}{4}} = \rho\sqrt{\frac{n}{2}},$$

as illustrated by the vertex $v_0 = (\frac{1}{2}^n)$. For $n = 4$ and 5, D_n is the densest known sphere packing in $\mathbb{R}^n$ (cf. [32]). For $n = 4$ the Voronoi region is a 24-cell (see for example [16, p. 156]), and $G(D_4) = 13/120\sqrt{2} = 0.0766032 \cdots$, in agreement with (24). This number also agrees closely with the value (8) that Gersho obtained for this region by Monte Carlo integration. The values of $G(D_n)$ for $n \leq 9$ are plotted in Fig. 20. $G(D_n)$ takes its minimum value of $0.0755905 \cdots$ at $n = 6$ and then slowly increases to $1/12$ as $n \rightarrow \infty$.

E. Voronoi Regions for E_6, E_7, E_8

The vertices of fundamental simplexes for E_6, E_7, and E_8 are shown in Fig. 9. For E_8

$$|W(E_8)| = 2^{14} \cdot 3^5 \cdot 5^2 \cdot 7 = 696729600, \qquad d = 1,$$

$$\hat{v} = \frac{1}{1080}(5, 35, 55, 79, 109, 149, 209, 751),$$

$$I(V(0)) = \frac{929}{1620},$$

$$\mathrm{vol}(V(0)) = 1,$$

$$G(E_8) = \frac{929}{12960} = 0.0716821 \cdots. \tag{34}$$

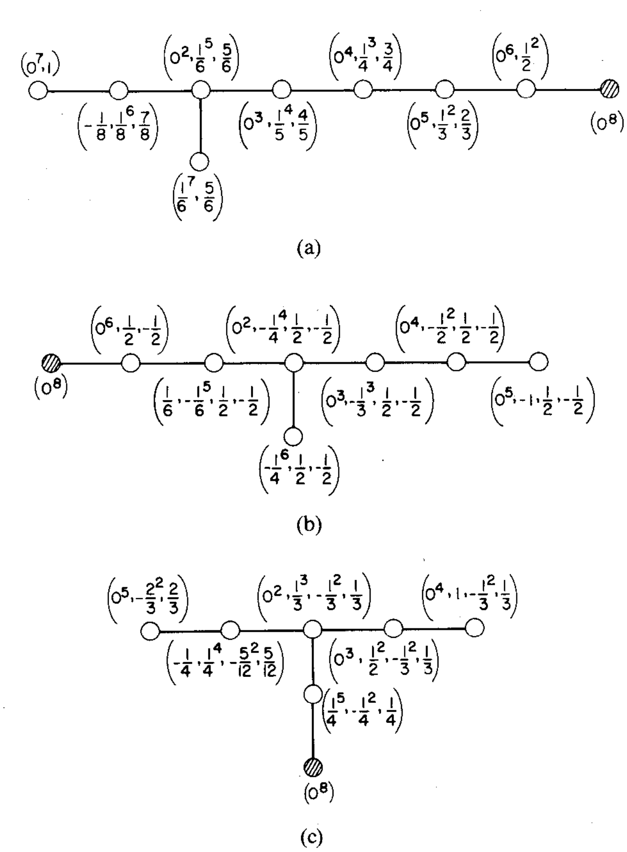

Fig. 9. Vertices of fundamental simplexes for (a) E_8, (b) E_7, and (c) E_6.

The Voronoi region $V(0)$ is an eight-dimensional polytope which is the reciprocal[5] to the Gosset polytope 4_{21} [16, p. 204].

Let N_i denote the number of i-dimensional faces of $V(0)$. Then from [16, p. 204] we have $N_0 = 19440$, $N_1 = 207360$, $N_2 = 483840$, $N_3 = 483840$, $N_4 = 241920$, $N_5 = 60480$, $N_6 = 6720$, and $N_7 = 240$. The 19440 vertices consist of 2160 at distance one from $\mathbf{0}$ and 17280 at distance $2\sqrt{2}/3$. The former are the images of the vertex $(0^7, 1)$ of the fundamental simplex under $W(E_8)$, and are at the maximum possible distance from E_8, while the latter are the images of the vertex $((1/6)^7, 5/6)$ under $W(E_8)$. Thus $R_c = 1 = \rho\sqrt{2}$. The other seven vertices of the fundamental simplex are not vertices of the Voronoi region.

For E_7, $|W(E_7)| = 2^{10} \cdot 3^4 \cdot 5 \cdot 7 = 2903040$, $d = 2$,

$$\hat{v} = -\frac{1}{96}(1, 5, 8, 12, 18, 30, -42, 42),$$

$$I(V(0)) = \frac{163}{288},$$

$$\mathrm{vol}(V(0)) = \sqrt{2},$$

$$G(E_7) = \frac{163}{2016} \cdot 2^{-1/7} = 0.0732306 \cdots. \tag{35}$$

The covering radius of E_7 is $R_c = \sqrt{3/2} = \rho\sqrt{3}$, as illustrated by the vertex $(0^5, -1, \frac{1}{2}, -\frac{1}{2})$.

[5] It is not difficult to give a direct proof of this statement; it also follows from Theorem 8 below.

For E_6, $|W(E_6)| = 2^7 \cdot 3^4 \cdot 5 = 51840$, $d = 3$,

$$\hat{v} = \frac{1}{42}(0,3,5,8,14,-14,-14,14),$$

$$I(V(0)) = \frac{15}{28},$$

$$\mathrm{vol}(V(0)) = \sqrt{3},$$

$$G(E_6) = \frac{5}{56 \cdot 3^{1/6}} = 0.0743467 \cdots. \quad (36)$$

The Voronoi regions for E_7 and E_6 are the reciprocals of the Gosset polytopes 2_{31} and 1_{22} described in [16, pp. 202–203]. The covering radius of E_6 is $R_c = 2/\sqrt{3} = \rho\sqrt{8/3}$, as illustrated by the vertices $(0^5, -2/3, -2/3, 2/3)$ and $(0^4, 1, -1/3, -1/3, 1/3)$.

F. Voronoi Region for D_n^*

In order to determine the Voronoi regions for the dual lattices A_n^* and D_n^* we shall use *Wythoff's construction*, as described in [13] and [16, § 11.6]. The idea is to construct new polytopes out of the spherical simplexes described in Section B, the vertices of the new polytope being indicated by drawing rings around certain nodes in the Coxeter–Dynkin diagram. More precisely, let $v_1, \cdots, v_n$ be the vertices of a spherical simplex for a Weyl group $W(\Lambda)$. If a single node of the diagram is ringed, say that corresponding to v_i, the vertices of the new polytope are the images of v_i under the Weyl group. If two or more nodes are ringed, say those corresponding to $v_i, v_j, \cdots$, the symbol represents a polytope whose vertices are the images under $W(\Lambda)$ of some interior point of the spherical subsimplex with vertices $v_i, v_j, \cdots$. We can adjust the metrical properties of the polytope (for example, equalize its edge lengths) by choosing this interior point suitably. Some one-, two-, and three-dimensional examples are shown in Fig. 10; others may be found in [13] and [16].

We now use this construction to find the Voronoi region for D_n^*, $n \geq 3$. In Section III-A we saw (using the second definition) that D_n^* is the union of the sets $(2\mathbb{Z})^n$ and $(1^n) + (2\mathbb{Z})^n$. The closest points to the origin from the first set consist of $2n$ points of the form $(\pm 2, 0^{n-1})$, and the closest from the second set consist of 2^n points of the form $(\pm 1^n)$. The Voronoi region $V(0)$ is the intersection of the Voronoi regions determined by these two sets. The first of these, P say, is a cube centered at zero with vertices $(\pm 1^n)$. The second, Q say, is a generalized octahedron with vertices $(\pm n/2, 0^{n-1})$. Furthermore Q can be obtained by reciprocating P in a sphere of radius $\rho = \sqrt{n/2}$ centered at the origin.

Thus the Voronoi region $V(0)$ is the intersection of P and a reciprocal polytope $Q = P^*$. In other words $V(0)$ is obtained by *truncating* P in the manner described in [16, p. 147], and is therefore specified by ringing one or two nodes of the Coxeter—Dynkin diagram (Fig. 4(b)) for the spherical simplex of P ([13], [16, § 8.1 and § 11.7]).

The radii R_j (defined in Section II-H) for the cube P are given by $R_j = \sqrt{n-j}$ ([16, p. 295]). If n is even the radius ρ of the sphere of reciprocation is equal to $R_{n/2}$, and we must ring the node labeled $n/2$ in Fig. 4(b). If n is odd ρ lies between $R_{(n-1)/2}$ and $R_{(n+1)/2}$ and both nodes $(n-1)/2$ and $(n+1)/2$ must be ringed. We have therefore established the following theorem.

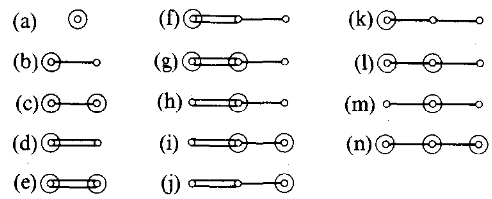

Fig. 10. Examples of polytopes obtained by Wythoff's construction: (a) edge, (b) triangle, (c) hexagon, (d) square, (e) octagon, (f) cube, (g) truncated cube, (h) cuboctahedron, (i) truncated octahedron, (j) octahedron, (k) tetrahedron, (l) truncated tetrahedron, (m) octahedron (again), and (n) truncated octahedron (again).

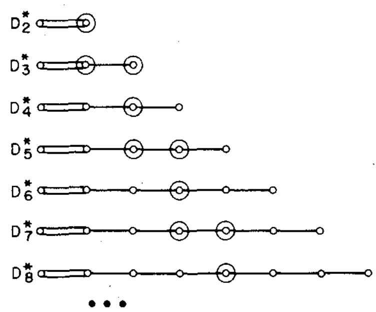

Fig. 11. Voronoi regions for the lattices D_n^*.

Theorem 6: The Voronoi region around the origin of the lattice D_n^* is the polytope defined by the diagrams in Fig. 11.

The coordinates for $\beta(n,k)$ and $\delta(n,k)$ given below show that the edge-lengths of the Voronoi regions are all equal. In Coxeter's notation [16, p. 146] the Voronoi region for D_{2t}^* is

$$\begin{Bmatrix} 3 & 3 & \cdots & 3 & \\ 3 & 3 & \cdots & 3 & 4 \end{Bmatrix},$$

with $t-1$ threes in each row, and for D_{2t+1}^* it is

$$\left\{ 3 \begin{matrix} 3 & 3 & \cdots & 3 & \\ 3 & 3 & \cdots & 3 & 4 \end{matrix} \right\}$$

with $t-1$ threes in the top and bottom rows.

We shall determine the second moments of these Voronoi regions recursively, using Theorem 3. In order to do this it will be necessary to find the second moments of all the polytopes $\alpha(n,k)$, $\beta(n,k)$, $\gamma(n,k)$, and $\delta(n,k)$ defined in Fig. 12. In this notation the Voronoi region of D_n^* is (up to a scale factor) equal to $\beta(n, n/2)$ if n is even and to $\delta(n,(n-1)/2)$ if n is odd. Let $R_\alpha(n,k)$, $V_\alpha(n,k)$, and $U_\alpha(n,k)$ denote respectively the circumradius, volume, and unnormalized second moment about the center of $\alpha(n,k)$, with a similar notation for $\beta(n,k)$, $\gamma(n,k)$, and $\delta(n,k)$.

For the vertices of the polytope $\alpha(n,k)$ it is convenient to take the points in $\mathbb{R}^{n+1}$ whose coordinates are all

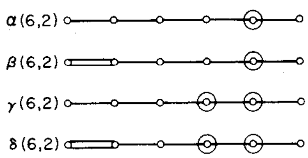

Fig. 12. Polytopes $\alpha(n,k)$, $\beta(n,k)$, $\gamma(n,k)$, and $\delta(n,k)$. In general $\alpha(n,k)$ has n nodes with the kth node from the right ringed, and $\gamma(n,k)$ has n nodes with the kth and $(k+1)$st ringed (except that $\gamma(n,0)=\alpha(n,1)$ and $\gamma(n,n)=\alpha(n,n)$). $\beta(n,k)$ and $\delta(n,k)$ are the same as $\alpha(n,k)$ and $\gamma(n,k)$, respectively, except that the left branch is a double bond. By convention $\alpha(0,0)$ and $\gamma(0,0)$ represent a point.

permutations of $(0^{n-k+1}, 1^k)$ [16, pp. 157–158]. The centroid of $\alpha(n,k)$ is the point

$$\frac{k}{n+1}(1^n),$$

and so the circumradius is

$$R_\alpha(n,k)=\sqrt{\frac{k(n-k+1)}{n+1}}.$$

Similarly

$\beta(n,k)$ has vertices $(0^{n-k+1}, \pm 1^k)$, $R_\beta(n,k)=\sqrt{k}$,

$\gamma(n,k)$ has vertices $(0^{n-k}, 1, 2^k)$,

$$R_\gamma(n,k)=\sqrt{\frac{4k(n-k)+n}{n+1}},$$

$\delta(n,k)$ has vertices $(0^{n-k}, \pm 1, \pm 2^k)$,

$$R_\delta(n,k)=\sqrt{4k+1}.$$

(These polytopes appear with different names in [17].) Each of these polytopes has two kinds of cells obtained by deleting either the left or the right node of its diagram [16, § § 7.6, 11.6, 11.7]. For example deleting the left node of the $\alpha(n,k)$ diagram produces an $\alpha(n-1,k-1)$, while deleting the right node produces an $\alpha(n-1,k)$. Thus in general $\alpha(n,k)$ has cells of type $\alpha(n-1,k-1)$ and $\alpha(n-1,k)$. (If $k=0$ the first type is absent, while if $k=n$ the second type is absent.) The number of cells of each type is given by the ratio of the orders of the underlying Weyl groups (obtained by ignoring the rings on the diagram). Thus the number of $\alpha(n-1,k-1)$-type cells of an $\alpha(n,k)$ is

$$\frac{|[3^{n-1}]|}{|[3^{n-2}]|}=\frac{(n+1)!}{n!}=n+1.$$

This is also the number of $\alpha(n-1,k)$-type cells. We represent this process of finding the cells by the graph shown in Fig. 13.

We can now apply Theorem 3 to $\alpha(n,k)$, obtaining

$$V_\alpha(n,k)=\frac{(n+1)h_L}{n}V_\alpha(n-1,k-1)+\frac{(n+1)h_R}{n}V_\alpha(n-1,k),$$

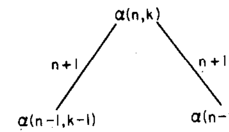

Fig. 13. The polytope $\alpha(n,k)$ has $n+1$ cells of type $\alpha(n-1,k-1)$ and $n+1$ of type $\alpha(n-1,k)$.

$$\begin{aligned}U_\alpha(n,k)=&\frac{(n+1)h_L}{n+2}\left(h_L^2V_\alpha(n-1,k-1)\right.\\&\left.+U_\alpha(n-1,k-1)\right)\\&+\frac{(n+1)h_R}{n+2}\left(h_R^2V_\alpha(n-1,k)+U_\alpha(n-1,k)\right),\end{aligned}$$

where

$$h_L^2=R_\alpha(n,k)^2-R_\alpha(n-1,k-1)^2=\frac{(n-k+1)^2}{n(n+1)},$$

$$h_R^2=R_\alpha(n,k)^2-R_\alpha(n-1,k)^2=\frac{k^2}{n(n+1)},$$

the subscripts on h standing for left and right. If we write

$$V_\alpha(n,k)=v_\alpha(n,k)\frac{\sqrt{n+1}}{n!}, \tag{37}$$

$$U_\alpha(n,k)=u_\alpha(n,k)\frac{\sqrt{n+1}}{(n+2)!}, \tag{38}$$

then v_α and u_α are integers satisfying the recurrences

$$v_\alpha(n,k)=(n-k+1)v_\alpha(n-1,k-1)+kv_\alpha(n-1,k), \tag{39}$$

for $n\ge 2$ and $1\le k\le n$, with $v_\alpha(n,0)=v_\alpha(n,n+1)=0$ for $n\ge 1$, and $v_\alpha(1,1)=1$, and

$$\begin{aligned}u_\alpha(n,k)=&(n-k+1)^3v_\alpha(n-1,k-1)\\&+k^3v_\alpha(n-1,k)\\&+(n-k+1)u_\alpha(n-1,k-1)\\&+ku_\alpha(n-1,k),\end{aligned} \tag{40}$$

for $n\ge 2$ and $1\le k\le n$, with $u_\alpha(n,0)=u_\alpha(n,n+1)=0$ for $n\ge 1$, and $u_\alpha(1,1)=1$. The first few values of v_α and u_α are shown in Table III. With the help of [44] the v_α may be identified as the Eulerian numbers [41, p. 215], and are given by

$$v_\alpha(n,k)=\sum_{j=0}^{k}(-1)^j\binom{n+1}{j}(k-j)^n. \tag{41}$$

There is a more complicated formula for $u_\alpha(n,k)$ which we omit.

Similarly for the polytope $\beta(n,k)$ we have the graph shown in Fig. 14, and writing

$$V_\beta(n,k)=v_\beta(n,k)\frac{2^n}{n!}, \tag{42}$$

$$U_\beta(n,k)=u_\beta(n,k)\frac{2^n}{(n+2)!}, \tag{43}$$

TABLE III
THE FIRST FEW VALUES OF $v_\alpha(n,k)$, $u_\alpha(n,k)$, $v_\beta(n,k)$, AND $u_\beta(n,k)$. THE DIAGONALS CORRESPOND TO $k = 1, 2, \cdots$.

n							
6	1	57	302	302	57	1	
5	1	26	66	26	1		
4	1	11	11	1			
3	1	4	1				$v_\alpha(n,k)$
2	1	1					
1	1						

n							
6	6	1158	8916	8916	1158	6	
5	5	400	1290	400	5		
4	4	116	116	4			
3	3	24	3				$u_\alpha(n,k)$
2	2	2					
1	1						

n							
6	1	58	360	662	719	720	
5	1	27	93	119	120		
4	1	12	23	24			
3	1	5	6				$v_\beta(n,k)$
2	1	2					
1	1						

n							
6	12	2568	28848	69624	80388	80640	
5	10	950	5490	8250	8400		
4	8	312	880	960			
3	6	84	120				$u_\beta(n,k)$
2	4	16					
1	2						

we obtain the recurrences

$$v_\beta(n,k) = nv_\beta(n-1,k-1) + kv_\alpha(n-1,k), \tag{44}$$

for $n \ge 2$ and $1 \le k \le n$, with $v_\beta(n,0) = 0$ for $n \ge 1$, and $v_\beta(1,1) = 1$, and

$$u_\beta(n,k) = k^3(n+1)v_\alpha(n-1,k) + ku_\alpha(n-1,k) + n^2(n+1)v_\beta(n-1,k-1) + nu_\beta(n-1,k-1), \tag{45}$$

for $n \ge 2$ and $1 \le k \le n$, with $u_\beta(n,0) = 0$ for $n \ge 1$, $u_\beta(1,1) = 2$ (see Table III). Furthermore one can show by induction that

$$v_\beta(n,k) = \sum_{i=1}^{k} v_\alpha(n,i), \tag{46}$$

which implies $v_\beta(n,n) = n!$. Since the $v_\alpha(n,k)$ satisfy $v_\alpha(n,k) = v_\alpha(n, n-k+1)$ it follows that

$$v_\beta(2t,t) = \frac{1}{2}(2t)! \tag{47}$$

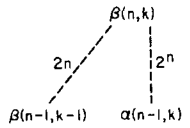

Fig. 14. $\beta(n,k)$ has $2n$ cells of type $\beta(n-1,k-1)$ and 2^n of type $\alpha(n-1,k)$. (We use broken lines here to make the structure of Figs. 15 and 16 more visible.)

For $\gamma(n,k)$ and $\delta(n,k)$ we have a pair of graphs similar to Figs. 13 and 14 (simply replace α by γ and β by δ in Figs. 13 and 14). As before we set

$$V_\gamma(n,k) = v_\gamma(n,k)\frac{\sqrt{n+1}}{n!},$$

$$U_\gamma(n,k) = u_\gamma(n,k)\frac{\sqrt{n+1}}{(n+2)!},$$

$$V_\delta(n,k) = v_\delta(n,k)\frac{2^n}{n!},$$

$$U_\delta(n,k) = u_\delta(n,k)\frac{2^n}{(n+2)!},$$

and obtain the recurrences

$$v_\gamma(n,k) = (2n-2k+1)v_\gamma(n-1,k-1) + (2k+1)v_\gamma(n-1,k), \tag{48}$$

for $n \ge 1$ and $0 \le k \le n$, with $v_\gamma(n,-1) = v_\gamma(n,n+1) = 0$ for $n \ge 0$, and $v_\gamma(0,0) = 1$;

$$u_\gamma(n,k) = (2n-2k+1)^3 v_\gamma(n-1,k-1) + (2k+1)^3 v_\gamma(n-1,k) + (2n-2k+1)u_\gamma(n-1,k-1) + (2k+1)u_\gamma(n-1,k), \tag{49}$$

for $n \ge 1$ and $0 \le k \le n$, with $u_\gamma(n,-1) = u_\gamma(n,n+1) = 0$ for $n \ge 0$, and $u_\gamma(0,0) = 0$;

$$v_\delta(n,k) = 2nv_\delta(n-1,k-1) + (2k+1)v_\gamma(n-1,k), \tag{50}$$

for $n \ge 1$ and $0 \le k \le n$, with $v_\delta(n,-1) = 0$ for $n \ge 0$, and $v_\delta(0,0) = 1$;

$$u_\delta(n,k) = (2k+1)^3(n+1)v_\gamma(n-1,k) + (2k+1)u_\gamma(n-1,k) + 8n^2(n+1)v_\delta(n-1,k-1) + 2nu_\delta(n-1,k-1), \tag{51}$$

for $n \ge 1$ and $0 \le k \le n$, with $u_\delta(n,-1) = 0$ for $n \ge 0$, and $u_\delta(0,0) = 0$ (see Table IV). Also

$$v_\gamma(n,k) = \sum_{j=0}^{k} (-1)^j \binom{n+1}{j}(2k+1-2j)^n,$$

$$v_\delta(n,k) = \sum_{i=0}^{k} v_\gamma(n,i),$$

$$v_\delta(n,n) = 2^n n!, \quad v_\delta(2t+1,t) = 2^{2t}(2t+1)!. \tag{52}$$

TABLE IV
$v_\gamma(n,k)$, $u_\gamma(n,k)$, $v_\delta(n,k)$, AND $u_\delta(n,k)$. THE DIAGONALS CORRESPOND TO $k = 0, 1, \cdots$.

n							
5	1	237	1682	1682	237	1	
4	1	76	230	76	1		
3	1	23	23	1			
2	1	6	1				$v_\gamma(n,k)$
1	1	1					
0	1						

n							
5	5	10065	124330	124330	10065	5	
4	4	2416	10520	2416	4		
3	3	477	477	3			
2	2	60	2				$u_\gamma(n,k)$
1	1	1					
0	0						

n							
5	1	238	1920	3602	3839	3840	
4	1	77	307	383	384		
3	1	24	47	48			
2	1	7	8				$v_\delta(n,k)$
1	1	2					
0	1						

n							
5	10	20840	369740	954120	1074490	1075200	
4	8	5224	41240	61048	61440		
3	6	1140	3654	3840			
2	4	188	256				$u_\delta(n,k)$
1	2	16					
0	0						

The j-dimensional faces of $\alpha(n,k),\cdots,\delta(n,k)$ for any j can be found from Figs. 15 and 16.

The special cases we are most interested in are $\beta(2t,t)$ and $\delta(2t+1,t)$, the Voronoi regions for D_{2t}^* and D_{2t+1}^* respectively. For D_{2t}^* we have

$$\mathrm{vol}\,(V(0)) = v_\beta(2t,t)\frac{2^{2t}}{(2t)!} = 2^{2t-1}, \quad \text{from (47)},$$

$$U(V(0)) = u_\beta(2t,t)\frac{2^{2t}}{(2t+2)!},$$

$$G(D_{2t}^*) = \frac{u_\beta(2t,t)}{2^{2-1/t}t(2t+2)!},$$

$$\rho = 1, \tag{53}$$

and covering radius

$$R_c = R_\beta(2t,t) = \sqrt{t} = \rho\sqrt{t}.$$

For this version of D_{2t+1}^* (which differs by a scale factor

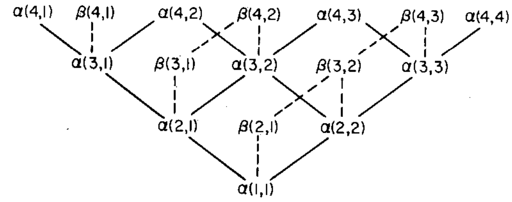

Fig. 15. Interconnections between the $\alpha(n,k)$ and $\beta(n,k)$.

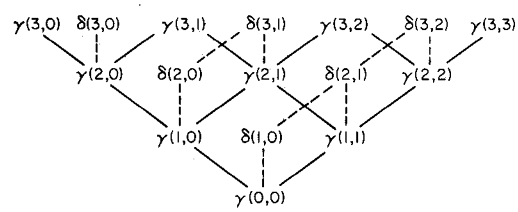

Fig. 16. Interconnections between the $\gamma(n,k)$ and $\delta(n,k)$.

from the definitions given in Section III-A) we have

$$\mathrm{vol}\,(V(0)) = v_\delta(2t+1,t)\frac{2^{2t+1}}{(2t+1)!} = 2^{4t+1}, \quad \text{from (52)},$$

$$U(V(0)) = u_\delta(2t+1,t)\frac{2^{2t+1}}{(2t+3)!},$$

$$G(D_{2t+1}^*) = \frac{u_\delta(2t+1,t)}{(2t+1)(2t+3)!2^{f(t)}}, \tag{54}$$

where

$$f(t) = \frac{2(2t^2+5t+1)}{2t+1},$$

$$\rho = \sqrt{3} \quad (\text{if } t = 1), \qquad \rho = 2 \quad (\text{if } t > 1),$$

$$R_c = R_\delta(2t+1,t) = \sqrt{4t+1}$$

$$= \rho\sqrt{\frac{5}{3}} \quad (\text{if } t = 1), \qquad \rho\sqrt{t+\frac{1}{4}} \quad (\text{if } t > 1).$$

For example $D_3^* \cong A_3^*$ is the body-centered cubic lattice, the Voronoi region is a truncated octahedron (see [22, page 294 and anaglyph XI], [24, fig. 4], and [33, p. 129]), and $G(D_3^*) = 19/192\sqrt[3]{2}$ (see (7) and Section II-G). Also

$$G(D_4^*) = 13/120\sqrt{2} = G(D_4),$$

$$G(D_5^*) = \frac{2641}{23040 \cdot 2^{3/5}} = 0.0756254\cdots, \tag{55}$$

$$G(D_6^*) = \frac{601 \cdot 2^{1/3}}{10080} = 0.0751203\cdots. \tag{56}$$

The values of $G(D_n^*)$ are plotted in Fig. 20. The minimum value is $0.0746931\cdots$ at $n = 9$.

G. Voronoi Region for A_n^*

Theorem 7: The Voronoi region for the lattice A_n^* is the polytope P_n defined in Fig. 17. If we rescale A_n^* by multiplying it by $n+1$, the vertices of the Voronoi region may be taken to be the images of the point

$$\sigma = \left(-\frac{n}{2}, -\frac{n-2}{2}, -\frac{n-4}{2}, \cdots, \frac{n-2}{2}, \frac{n}{2}\right)$$

under the action of the Weyl group $W(A_n)$.

Since σ is sometimes referred to as the Weyl vector for A_n (see [10]), it is appropriate to call P_n the *Weyl polytope* of A_n. The case $n = 4$ of this theorem may be found in [15, pp. 72–73].

Sketch of Proof: It is easy to check that σ is equidistant from the walls of the fundamental simplex S for A_n; i.e. that σ is the incenter of S. Let P be the convex hull of the images of σ under $W(A_n)$. Since the walls of S are reflecting hyperplanes for $W_a(A_n)$, P and its images under $W_n(A_n)$ tile $\mathbb{R}^n$. Thus P is the Voronoi region for some lattice $\Lambda \subseteq A_n^*$. But Λ must contain all the points (28), since these are the images of $\mathbf{0}$ in the walls of P. Since these points span A_n^*, $\Lambda = A_n^*$.

The second moment of P_n may be found as follows. First, the covering radius of A_n^*, $R_c(n)$ say, is the circumradius of P_n, which is

$$R_c(n) = \sqrt{\sigma \cdot \sigma} = \left\{\frac{1}{2}\binom{n+2}{3}\right\}^{1/2}$$
$$= \rho\sqrt{\frac{n+2}{3}}, \tag{57}$$

since now $\rho = \sqrt{n(n+1)/4}$, and the volume of P_n is

$$V_n = (n+1)^{n-1/2} \text{ from (27).} \tag{58}$$

Let $I_n = I(P_n)$ be the normalized second moment. A typical cell of P_n is obtained by deleting say the rth node from the left in Fig. 17, and is a prism $P_r \times P_s$ with $r + s = n - 1$ (see Fig. 18). The number of such faces is

$$\frac{|W(A_n)|}{|W(A_r)||W(A_S)|} = \binom{n+1}{r+1}. \tag{59}$$

Furthermore $I(P_r \times P_s) = I_r + I_s$.

Let h_{rs} be the height of the perpendicular from the center of P_n to a typical face $P_r \times P_s$. Then (see Fig. 19)

$$h_{rs}^2 = R_c(r+s+1)^2 - R_c(r)^2 - R_c(s)^2$$
$$= \frac{(r+1)(s+1)(n+1)}{4}, \quad \text{using (57).}$$

We may now apply Theorem 3, to obtain

$$I_nV_n = \frac{1}{n+2}\sum_{r=0}^{n-1}\binom{n+1}{r+1}h_{rs}V_rV_s\left(h_{rs}^2 + I_r + I_s\right)$$

(with $r + s = n - 1$), which, if we write $J_n = I_{n-1}/n$, becomes

$$J_n = \frac{1}{2(n+1)n^{n-1}}\sum_{r=1}^{n-1}\binom{n}{r}r^rs^s\left(\frac{n}{4} + \frac{J_r}{s} + \frac{J_s}{r}\right),$$

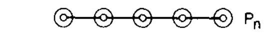

Fig. 17. Voronoi region $P_n = V(0)$ for A_n^*. There are n nodes, all ringed.

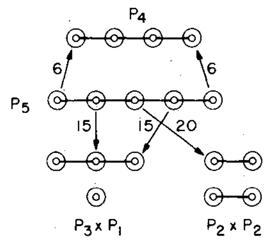

Fig. 18. The three types of cells of P_5.

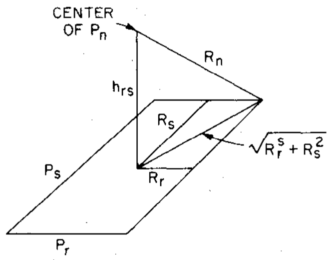

Fig. 19. Calculation of height h_{rs} of perpendicular from center of P_n to cell $P_r \times P_s$.

where $r + s = n - 2$. Using Abel's identity [42, section 1.5] to simplify the first term, this becomes

$$J_n = \frac{n!}{8(n+1)n^{n-2}}\sum_{k=0}^{n}\frac{n^k}{k!} - \frac{n^2}{4(n+1)}$$
$$+ \frac{1}{n+1}\sum_{r=1}^{n-1}\binom{n}{r}\left(\frac{r}{n}\right)^r\left(\frac{n-r}{n}\right)^{n-r-1}J_r \tag{60}$$

for $n \geq 2$, with $J_1 = 0$. The first few values are as follows:

n:	1	2	3	4	5	6	7
J_n:	0	$\frac{1}{12}$	$\frac{5}{18}$	$\frac{19}{32}$	$\frac{389}{375}$	$\frac{1045}{648}$	$\frac{78077}{33614}$.

Finally, the dimensionless second moment of the Voronoi region of A_n^* is

$$G(A_n^*) = \frac{J_{n+1}}{n(n+1)^{1-(1/n)}}. \tag{61}$$

The values for $n \leq 9$ are plotted in Fig. 20. The curve is extremely flat, the minimum value of $0.0754913 \cdots$ occurring at $n = 16$.

H. When is the Voronoi Region Determined by the First Layer of the Lattice?

We have seen in the Corollary to Theorem 5 that for a root lattice the walls of the Voronoi region are determined solely by the minimum vectors of the lattice. To give a precise statement of this property for an arbitrary lattice Λ, let us write $\Lambda = \Lambda_0 \cup \Lambda_1 \cup \Lambda_2 \cup \cdots$, where Λ_i, the ith *layer* from the origin, is chosen so that $\boldsymbol{u} \cdot \boldsymbol{u}$ is a constant λ_i (say) for all $\boldsymbol{u} \in \Lambda_i$, and $0 = \lambda_0 < \lambda_1 < \lambda_2 < \cdots$. We say that the Voronoi region is determined by the first layer of the lattice if the walls of the Voronoi region around the origin, $V(0)$, are bounded by the hyperplanes

$$\boldsymbol{x} \cdot \boldsymbol{u} = \tfrac{1}{2}\lambda_1, \qquad \text{for } \boldsymbol{u} \in \Lambda_1. \tag{62}$$

If this property holds then there is a simple description of the Voronoi region.

Theorem 8: If the Voronoi region $V(0)$ is determined by the first layer of the lattice, then $V(0)$ is the reciprocal of the vertex figure of Λ at the origin. Equivalently, $V(0)$ is (on a suitable scale) the reciprocal of the polytope with vertices Λ_1.

Proof: This follows immediately from the definitions of vertex figure and reciprocal polytope—see [16].

The final two theorems give sufficient conditions for this property to hold.

Theorem 9: Suppose that (i) $\Lambda_r \subseteq \Lambda_1 + \Lambda_1 + \cdots + \Lambda_1$ (r times) and (ii) $r\lambda_1 \le \lambda_r$, for all $r = 1, 2, \cdots$. Then the Voronoi region is determined by the first layer.

Condition (i) states that Λ_1 spans Λ, and moreover does it economically in the sense that any vector in Λ_r is the sum of not more than r vectors of Λ_1. In practice this condition is very easily checked by induction. An important class of lattices satisfying (i) are those obtained by applying Construction A of [32] or [45] to a linear binary code with minimum distance ≤ 4, which is spanned by the codewords of minimum weight, and which if $d < 4$ has the additional property that no coordinate of the code is always **0**.

Proof of Theorem 9: Suppose the contrary, so that there is a point $\boldsymbol{u} \in \Lambda_r$ with $r > 1$ and a point $\boldsymbol{x} \in \mathbb{R}^n$ such that

$$\boldsymbol{x} \cdot \boldsymbol{u} > \tfrac{1}{2}\lambda_r$$

but

$$\boldsymbol{x} \cdot \boldsymbol{v} \le \tfrac{1}{2}\lambda_1, \qquad \text{for all } \boldsymbol{v} \in \Lambda_1.$$

From (i), $\boldsymbol{u} = \Sigma n_i \boldsymbol{v}_i$ with $\boldsymbol{v}_i \in \Lambda_1$, $n_i > 0$ and $\Sigma n_i \le r$. Then

$$\boldsymbol{x} \cdot \boldsymbol{u} = \Sigma n_i (\boldsymbol{x} \cdot \boldsymbol{v}_i) \le \tfrac{1}{2}\lambda_1 \Sigma n_i$$
$$\le \tfrac{1}{2} r \lambda_1 \le \tfrac{1}{2}\lambda_r,$$

a contradiction.

Theorem 9 can be used to give an alternative proof that any root lattice has the property. On the other hand the dual lattices A_n^* for $n \ge 3$ and D_n^* for $n \ge 5$ do not, as the previous section demonstrated, nor does the Leech lattice in 24 dimensions [9], [32]. In fact one can show that the Voronoi region of the Leech lattice is determined just by the first two layers: in other words the Voronoi region has $196560 + 16773120 = 16969680$ cells.

A second test is the following.

Theorem 10 (A. Gersho, private communication): Let V_1 be the intersection of the half-planes defined by (62). If $\boldsymbol{x} \cdot \boldsymbol{x} \le \frac{1}{4}\lambda_2$ holds for all $\boldsymbol{x} \in V_1$, then V_1 is the Voronoi region.

TABLE V
DIMENSIONLESS SECOND MOMENT $G(\Lambda)$.

n	sphere bound	best lattice known Λ	best lattice known $G(\Lambda)$	Zador bound
1	.0833	A_1	.0833	.500
2	.0796	A_2	.0802	.159
3	.0770	A_3^*	.0785	.116
4	.0750	D_4	.0766	.100
5	.0735	D_5^*	.0756	.091
6	.0723	E_6	.0743	.086
7	.0713	E_7	.0732	.082
8	.0704	E_8	.0717	.080
9	.0697	D_9^*	.0747	.078
10	.0691	D_{10}^*	.0747	.076

Proof: Take any $\boldsymbol{x} \in V_1$, $\boldsymbol{v} \in \Lambda_2 \cup \Lambda_3 \cup \cdots$. Then $\boldsymbol{x} \cdot \boldsymbol{v} \le \|\boldsymbol{x}\| \, \|\boldsymbol{v}\| \le \frac{1}{2}\sqrt{\lambda_2}\sqrt{\lambda_2} = \frac{1}{2}\lambda_2$, so $\boldsymbol{x} \in V(0)$.

IV. COMPARISON OF QUANTIZERS

Comparing the different lattices analyzed in this section we see that the best quantizers found so far in dimensions 1–10 are the following:

dimension	lattice	dimension	lattice
1	$A_1 (\cong A_1^*)$	6	E_6
2	$A_2 (\cong A_2^*)$	7	E_7
3	$A_3^* (\cong D_3^*)$	8	$E_8 (= E_8^*)$
4	$D_4 (\cong D_4^*)$	9	D_9^*
5	D_5^*	10	D_{10}^* .

The values of the dimensionless second moment $G(\Lambda)$, which is our measure of the mean-squared quantization error per symbol, are shown in Table V and Fig. 20, together with Zador's bounds (3). It is known that A_1 and A_2 are optimal, and it is tempting to make the following conjecture.

Conjecture

The best *lattice* quantizer in $\mathbb{R}^n$—that with the lowest $G(\Lambda)$—is the dual of the densest lattice packing.

Certainly E_6^*, E_7^*, and the Leech lattice should be investigated.

It is worth drawing attention to the remarkably low value of the mean-squared error for E_8 (see Fig. 20). Furthermore there is a fast algorithm [12] available for performing the quantization with this lattice (and in fact for any of the lattices described here).

Note added in proof: It has recently been shown that the body-centered cubic lattice A_3^* is the optimal three-dimensional lattice quantizer for uniformly distributed data: see E. S. Barnes and N. J. A. Sloane, "The optimal lattice

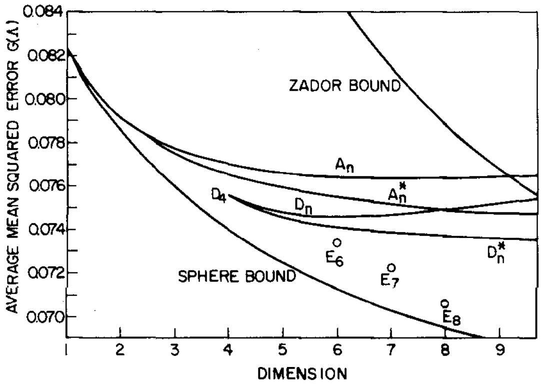

Fig. 20. Comparison of mean-squared quantization error per symbol, $G(\Lambda)$, for different lattices Λ in dimensions 1–9.

quantizer in three dimensions," *SIAM J. Discrete and Algebraic Methods*, to appear.

Acknowledgment

During the early stages of this work we were greatly helped by several discussions with Allen Gersho. Some of the calculations were performed on the MACSYMA system [35]. We should also like to thank E. S. Barnes and H. S. M. Coxeter for their comments on the manuscript.

References

[1] A. D. Alexandrow, *Konvexe Polyeder*. Berlin: Akademie-Verlag, 1958.

[2] E. S. Barnes, "Construction of perfect and extreme forms II," *Acta Arithmetica*, vol. 5, pp. 205–222, 1959.

[3] C. T. Benson and L. C. Grove, *Finite Reflection Groups*. Tarrytown-on-Hudson, NY: Bogden and Quigley, 1971.

[4] M. N. Bleicher, "Lattice coverings of n-space by spheres," *Can. J. Math.*, vol. 14, pp. 632–650, 1962.

[5] N. Bourbaki, *Groupes et Algèbres de Lie, Chapitres 4, 5 et 6*. Paris: Hermann, 1968.

[6] J. A. Bucklew, "Upper bounds to the asymptotic performance of block quantizers," *IEEE Trans. Inform. Theory*, vol. IT-27, no. 5, pp. 577–581, Sept. 1981.

[7] J. A. Bucklew and G. L. Wise, "A note on multidimensional asymptotic quantization theory," *Proc. 18th Allerton Conf. on Commun., Control, and Computing*, 1980, pp. 454–463.

[8] J. W. S. Cassels, *An Introduction to the Geometry of Numbers*. New York: Springer-Verlag, 1971.

[9] J. H. Conway, R. A. Parker, and N. J. A. Sloane, "The covering radius of the Leech lattice," *Proc. Royal Soc.*, 1982, to be published.

[10] J. H. Conway and L. Queen, "On computing the characters of Lie groups," in preparation.

[11] J. H. Conway and N. J. A. Sloane, "On the enumeration of lattices of determinant one," *J. Number Theory*, to be published.

[12] ——, "Fast quantizing and decoding algorithms for lattice quantizers and codes," *IEEE Trans. Inform. Theory*, this issue, pp. 227–232.

[13] H. S. M. Coxeter, "Wythoff's construction for uniform polytopes," *Proc. London Math. Soc.*, Ser. 2, vol. 38, pp. 327–339, 1935; reprinted in [15].

[14] ——, "Extreme forms," *Can. J. Math.*, vol. 3, pp. 391–441, 1951.

[15] ——, *Twelve Geometric Essays*. Carbondale: Southern Illinois Univ., 1968.

[16] ——, *Regular Polytopes*. New York: Dover, 3rd ed., 1973.

[17] ——, "Polytopes in the Netherlands," *Nieuw Archief voor Wiskunde (3)*, vol. 26, pp. 116–141, 1978.

[18] H. S. M. Coxeter and W. O. J. Moser, *Generators and Relations for Discrete Groups*. New York: Springer-Verlag, 4th ed., 1980.

[19] H. M. Cundy and A. P. Rollett, *Mathematical Models*. Oxford: The Univ., 1961.

[20] E. L. Elte, "The semiregular polytopes of the hyperspaces," Doctor of Math. and Science Thesis, State-Univ. of Gronigen, The Netherlands, 13 May 1912.

[21] L. Fejes Tóth, "Sur la représentation d'une population infinie par un nombre fini d'éléments," *Acta Math. Acad. Sci. Hungar.*, vol. 10, pp. 299–304, 1959.

[22] ——, *Regular Figures*. Oxford: Pergamon, 1964.

[23] ——, *Lagerungen in der Ebene, auf der Kugel und im Raum*. New York: Springer-Verlag, 2nd ed., 1972.

[24] A. Gersho, "Asymptotically optimal block quantization," *IEEE Trans. Inform. Theory*, vol. IT-25, no. 4, pp. 373–380, July 1979.

[25] I. J. Good and R. A. Gaskins, "The centroid method of numerical integration," *Numer. Math.*, vol. 16, pp. 343–359, 1971.

[26] B. Grünbaum, *Convex Polytopes*. New York: Wiley, 1967.

[27] M. Hazewinkel *et al.*, "The ubiquity of Coxeter–Dynkin diagrams (an introduction to the A-D-E problem)," *Nieuw Archief voor Wiskunde* (3), vol. 25, pp. 257–307, 1977.

[28] D. Hilbert and S. Cohn-Vossen, *Geometry and The Imagination*. New York: Chelsea, 1952.

[29] A. Holden, *Shapes, Space, and Symmetry*. New York: Columbia Univ., 1971.

[30] J. E. Humphreys, *Introduction to Lie Algebras and Representation Theory*. New York: Springer-Verlag, 1972.

[31] G. Kaur, "Extreme quadratic forms for coverings in four variables," *Proc. Nat. Inst. Sci. India*, vol. 32A, pp. 414–417, 1966.

[32] J. Leech and N. J. A Sloane, "Sphere packing and error-correcting codes," *Can. J. Math.* vol. 23, pp. 718–745, 1971.

[33] A. L. Loeb, *Space Structures: Their Harmony and Counterpoint*. Reading, MA: Addison-Wesley, 1976.

[34] L. A. Lyusternik, *Convex Figures and Polyhedra*. New York: Dover, 1963.

[35] Mathlab Group, *MACSYMA Reference Manual*. Cambridge, MA: Lab. Comp. Sci., M.I.T., version 9, 1977.

[36] P. McMullen and G. C. Shephard, *Convex Polytopes and the Upper Bound Conjecture*, London Math. Soc. Lecture Note Series 3. Cambridge: The Univ., 1971.

[37] D. J. Newman, "The hexagon theorem," *IEEE Trans. Inform. Theory*, this issue, pp. 137–139.

[38] H. V. Niemeier, "Definite quadratische Formen der Dimension 24 und Diskriminante 1," *J. Number Theory*, vol. 5, pp. 142–178, 1973.

[39] O. T. O'Meara, *Introduction to Quadratic Forms*. New York: Springer-Verlag, 1971.

[40] A. Pugh, *Polyhedra: A Visual Approach*. Berkeley: Univ. of Calif., 1976.

[41] J. Riordan, *An Introduction to Combinatorial Analysis*. New York: Wiley, 1958.

[42] J. Riordan, *Combinatorial Identities*. New York: Wiley, 1968.

[43] J. Satterly, "The moments of inertia of some polyhedra," *Math. Gazette*, vol. 42, pp. 11–13, 1958.

[44] N. J. A. Sloane, *A Handbook of Integer Sequences*. New York: Academic, 1973.

[45] N. J. A. Sloane, "Binary codes, lattices and sphere packings," in *Combinatorial Surveys* (Proc. 6th British Combinatorial Conf.), P. J. Cameron, Ed. London and New York: Academic, 1977, pp. 117–164.

[46] N. J. A. Sloane, "Self-dual codes and lattices," in *Relations Between Combinatorics and Other Parts of Mathematics*, Proc. Symp. Pure Math., vol. 34, Providence RI: Amer. Math. Soc., 1979, pp. 273–308.

[47] N. J. A. Sloane, "Tables of sphere packings and spherical codes," *IEEE Trans. Inform. Theory*, vol. IT-27, no. 3, pp. 327–338, May 1981.

[48] B. M. Stewart, *Adventures among the Toroids*. Published by the author, 4494 Wausau Rd., Okemos, MI, 1970.

[49] G. Voronoi, "Récherches sur les paralléloèdres primitifs I, II," *J. reine angew. Math.*, vol. 134, pp. 198–287, 1908, and vol. 136, pp. 67–181, 1909.

[50] M. J. Wenninger, *Polyhedron Models*. Cambridge: The Univ., 1971.

[51] E. T. Whittaker and G. N. Watson, *A Course of Modern Analysis*. Cambridge: The Univ., 4th ed., 1963.

[52] Y. Yamada, S. Tazaki, and R. M. Gray, "Asymptotic performance of block quantizers with difference distortion measures," *IEEE Trans. Inform. Theory*, vol. IT-26, no. 1, pp. 6–14, Jan. 1980.

[53] P. Zador, "Topics in the asymptotic quantization of continuous random variables," *IEEE Trans. Inform. Theory*, this issue, pp. 139–149.